

## LETTERS

**Drought in Central and Southwest Asia: La Niña, the Warm Pool, and Indian Ocean Precipitation**

MATHEW BARLOW, HEIDI CULLEN, AND BRADFIELD LYON

*International Research Institute for Climate Prediction,\* Palisades, New York*

10 September 2001 and 9 November 2001

## ABSTRACT

Severe drought over the past three years (1998–2001), in combination with the effects of protracted socio-political disruption, has led to widespread famine affecting over 60 million people in central and southwest (CSW) Asia. Here both a regional and a large-scale mode of climate variability are documented that, together, suggest a possible forcing mechanism for the drought. During the boreal cold season, an inverse relationship exists between precipitation anomalies in the eastern Indian Ocean and CSW Asia. Suppression of precipitation over CSW Asia is consistent with interaction between local synoptic storms and wave energy generated by enhanced tropical rainfall in the eastern Indian Ocean. This regional out-of-phase precipitation relationship is related to large-scale climate variability through a subset of El Niño–Southern Oscillation (ENSO) events characterized by an enhanced signal in the warm pool region of the western Pacific Ocean. Both the prolonged duration of the 1998–2001 cold phase ENSO (La Niña) event and unusually warm ocean waters in the western Pacific appear to contribute to the severity of the drought.

**1. CSW Asia and ongoing drought**

Most of central and southwest (CSW) Asia is semiarid steppe receiving little precipitation with, nonetheless, much of the population directly reliant on agriculture. Precipitation occurs primarily during late winter and early spring, due to orographic capture of eastward-propagating midlatitude cyclones from the Atlantic Ocean and Mediterranean Sea (Martyn 1992). This year (2001) marks the third consecutive year of drought for a broad region centered on Iran, Afghanistan, and Pakistan (see time series in Fig. 1), with wet season (November–April) precipitation since 1998/99 at less than 55% of the long-term average.

**2. Monitoring: Synchronous large-scale and regional anomalies**

The recent drought period, 1998–2001, has also featured coherent patterns of large spatial scale in Novem-

ber–April anomalies of precipitation, sea surface temperatures (SST), and wind (Fig. 2), including a prolonged cold-phase El Niño–Southern Oscillation (ENSO) event. The general aspects of the recent western and central Pacific climate anomalies are similar to the typical November–April ENSO signature in SSTs (Rasmusson and Carpenter 1982; Ropelewski and Halpert 1989), precipitation (Ropelewski and Halpert 1987), and upper-level winds (Horel and Wallace 1981).

However, other regional features during this period are not generally noted as being La Niña-related, particularly the Indian Ocean precipitation extension (IPX) region; see box in Fig. 2a) of the positive anomalies in the west Pacific, the drought in CSW Asia, and the exceptionally warm SSTs in the western Pacific (Hoerling et al. 2001).

**3. Potential mechanism for drought***a. Regional: Indian Ocean Precipitation Extension (IPX) and tropical forcing*

The time series for the IPX index is shown as the line in Fig. 1, revealing an out-of-phase relationship with CSW Asia not only during the recent drought period but throughout the record. The spatial pattern of precipitation correlated to the IPX index (Fig. 3a) shows that this general inverse relationship, while modest in

\* International Research Institute for Climate Prediction Contribution Number IRI-PP/01/22.

*Corresponding author address:* Dr. Mathew Barlow, International Research Institute for Climate Prediction, P.O. Box 1000, Palisades, NY 10964.  
E-mail: mattb@iri.ldeo.columbia.edu

## CSW ASIA PRECIP AND INDIAN OCEAN PRECIP EXTENSION (IPX)

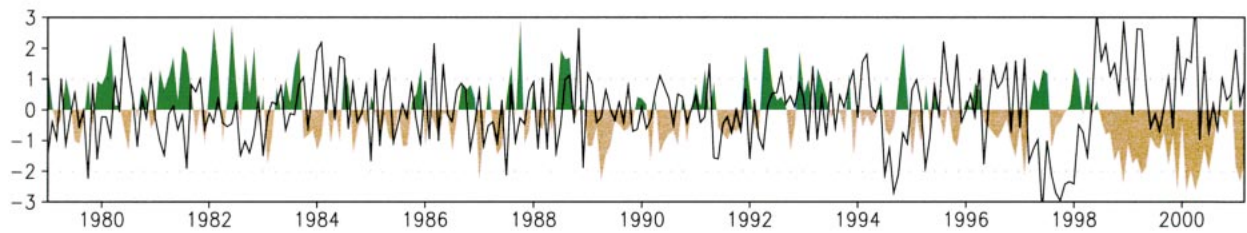


FIG. 1. CSW Asia drought evolution. Shown are the normalized monthly precipitation anomalies for CSW Asia drought region (shaded) and the IPX region (line) from Jan 1979 to Mar 2001. The drought region is  $30^{\circ}$ – $42^{\circ}$ N,  $42^{\circ}$ – $70^{\circ}$ E, and the IPX region is  $10^{\circ}$ S– $15^{\circ}$ N,  $90^{\circ}$ – $100^{\circ}$ E. Units are standard deviations; the CAMS-OPI data were used. Note persistence of drought (brown shading) since 1998.

magnitude, also has considerable similarity in position and extent to the recent drought period anomalies (Fig. 2a). The SST correlation (not shown) to the IPX index resembles an ENSO pattern with an enhanced signal in the warm pool region, as in the recent three winters. The covariance between the IPX and upper-level atmospheric circulation (Fig. 3a), consists primarily of

two westward-extended anticyclones poleward of the heating, favoring the winter hemisphere, again with considerable similarity to the drought period (Fig. 2a).

In the linear Gill–Matsuno model of tropical dynamics (Matsuno 1966; Gill 1980), the deep tropical latent heat release associated with the IPX precipitation would produce two baroclinic Rossby wave packets, symmetric about the equator, to the west of the heating. At upper levels these Rossby wave packets would be realized in the wind field as anticyclonic circulations. To illustrate

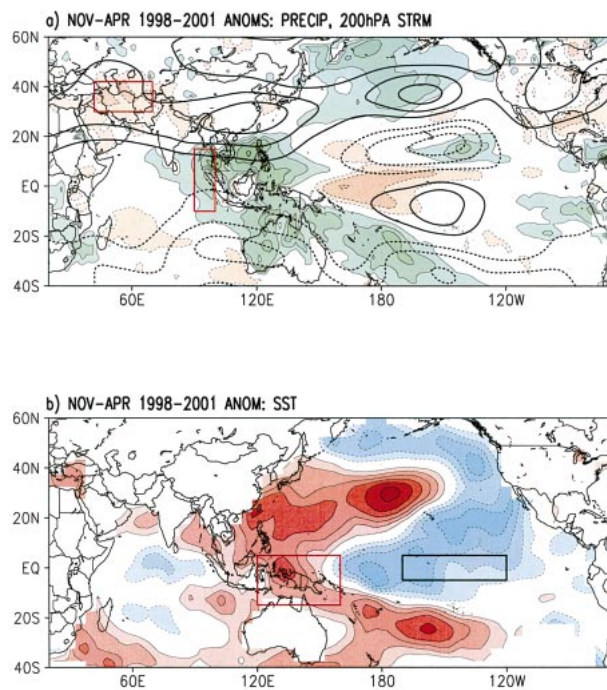


FIG. 2. Large-scale anomalies during drought period. Shown are standardized anomalies, Nov–Apr 1998–2001 for (a) precipitation (shaded) and 200-hPa streamfunction (contours), and (b) SST. For precipitation and SST, the contour interval is 0.5 monthly standard deviations. Streamfunctions (the nondivergent component of the wind) is shown in physical units (contour interval of  $3.5 \times 10^6 \text{ m}^2 \text{ s}^{-1}$ ) for comparison to model results. The boxes in (a) delineate the regions for the CSW Asia drought index and the index for ENSO (black box). The normalization here is done monthly, then averaged for Nov–Apr. The CAMS-OPI dataset (Janowiak and Xie 1999) was used for precipitation, the NCEP–NCAR reanalysis for streamfunction (Kalnay et al. 1996), and the reconstruction by Kaplan et al. for SSTs (Kaplan et al. 1998).

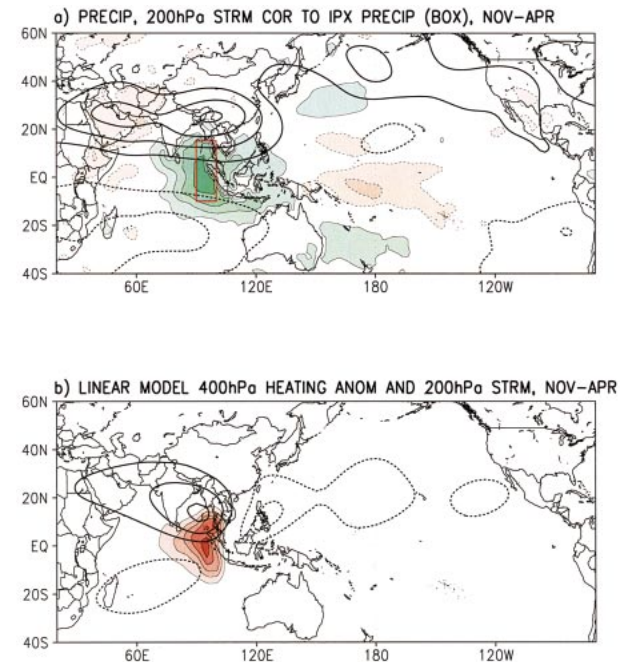


FIG. 3. Teleconnections to IPX. (a) Precipitation and 200-hPa streamfunction covariance with the IPX precipitation (red box) for 1979–96; (b) eastern Indian Ocean 400-hPa heating anomaly and linear model response in 200-hPa streamfunction. In (a), precipitation is shown as a correlation to IPX, the contour interval is 0.2, and the streamfunction is shown in physical units as a regression (contour interval is  $1.5 \times 10^6 \text{ m}^2 \text{ s}^{-1}$ ). Calculations were performed on monthly data, then averaged for Nov–Apr. In (b), the contour interval for heating is  $0.3 \text{ K day}^{-1}$  and the contour interval for the streamfunction is the same as in (a).

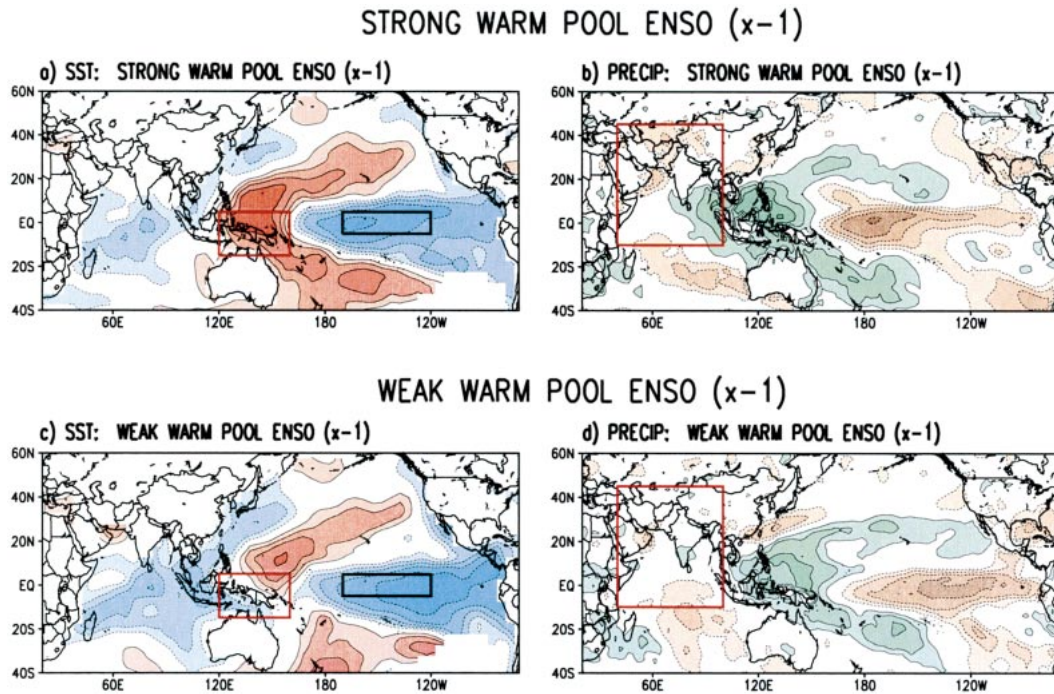


FIG. 4. ENSO warm pool stratification. Correlations with ENSO using the Niño-3.4 index [black box in (a)] for 1979–96, where the monthly contributions to the correlation are sorted into two equal-sized groups based on the strength of the warm pool SST anomalies in the western Pacific [red box in (a)]. All fields have been multiplied by  $-1$  to correspond to the cold phase of ENSO. The strong warm pool case is shown in the upper panels for (a) SST and (b) precipitation; similarly the weak warm pool case is shown in (c) and (d). A contour interval of 0.1 is used for all panels but does not directly correspond to correlation units; the weak and strong cases for each variable added together will yield the standard correction. Given the brief period of available global precipitation data, the stratification is done on the monthly data (with the final result averaged over Nov–Apr), and so any given ENSO can contribute to both the weak and strong cases. That this is of relevance to an entire event is demonstrated by the similarity of the 1998–2001 La Niña to the strong warm pool case. Both El Niños and La Niñas are considered; although the two phases are not completely symmetric, both display the noted relationships (with signs reversed), with the La Niña relationship more coherent.

this, the linear atmospheric response to deep heating in the IPX region is shown in Fig. 3b, in a steady-state linear model (Nigam et al. 1988). The anticyclonic anomalies of the Rossby wave response extend into CSW Asia with considerable similarity to the observed anomalies, and are consistent with suppression of synoptic activity. Interaction between the wave energy and the synoptic storms and local jet stream (centered at  $25^{\circ}$ – $30^{\circ}$ N in November–April) likely modifies the response, potentially reinforcing the anomaly (see review in Trenberth et al. 1998); this is consistent with the larger values and more zonal orientation of the observed anomalies.

#### *b. Large-scale: ENSO and the warm pool*

Although the IPX–CSW Asia precipitation relationship is not typically noted as part of the ENSO signal, there has also been an enhanced signal in the warm pool (red box in Fig. 2b) for both the recent La Niña and the SST correlations to the IPX. To test a possible relationship between the warm pool and changes in the

ENSO signal, we calculated standard correlations to the Niño-3.4 SST index of ENSO for both precipitation and SSTs, but with the monthly contributions to the correlations sorted into two equal-sized groups, based on the strength of the SST anomalies in the warm pool. That is, we stratified the ENSO relationships into two cases: a strong warm pool case, where the ENSO events occurred in conjunction with vigorous SST anomalies in the west Pacific; and a weak warm pool case, where the ENSO events occurred in conjunction with weak SST anomalies in the west Pacific. The results are shown in Fig. 4, with the signs reversed for comparison to La Niña. The recent drought period was not included in the calculations, to avoid bias by a single event.

The subset of ENSOs with a strong warm pool signal are associated with a vigorous extension of positive precipitation anomalies into the Indian Ocean (the IPX region) and negative anomalies over CSW Asia (Fig. 4b). The similarity between this rainfall pattern and the drought period rainfall (Fig. 2a) is striking. Although the magnitude of the pattern is modest, the difference in precipitation between the two cases for the Indian

Ocean–CSW Asia region (see red box in Fig. 4b) has high statistical significance: the probability that a random stratification of the ENSO correlation would result in as large a difference is less than 0.005 (using monthly data as with original calculation, therefore 108 samples over 18 yr). We have also stratified the correlations to the warm pool SST anomalies with respect to ENSO strength; the warm pool–IPX–CSW Asia relationship appears to be only present during active ENSO periods. Additionally, we have verified the warm pool–IPX relationship prior to the mid-1970s (the advent of satellite data and estimates of oceanic precipitation), by examining the warm pool stratification of ENSO correlation to upper-level winds for 1949–78.

#### 4. Discussion and implications

The similarity between the enhanced warm pool–La Niña composite and the climate anomalies of 1998–2001, in both regional and large-scale aspects, suggests that the prolonged, westward-concentrated La Niña during this period was a major factor in the CSW Asia drought. As the diagnosed linkages have been present throughout the available period of data, whereas the drought has been exceptionally harsh, we speculate that the severity of the drought is related to a combination of the prolonged duration of the recent La Niña and the unusually warm SSTs in the west Pacific, which may have enhanced the regional dynamics of the warm pool. Given the demise of the La Niña in early 2001, conditions may be favorable for a return toward normal in CSW Asia.

*Acknowledgments.* M. Barlow acknowledges support from the UCAR–IRI Postdoctoral Fellowship. H. Cullen acknowledges support from the NOAA Postdoctoral Program in Climate and Global Change. We thank C.

Ropelewski, P. Arkin, T. Barnston, and J. Zotter for useful discussions, and Sumant Nigam for the use of his linear model. IRI is supported by the NOAA Office of Global Programs, Columbia University, and the government of Taiwan.

#### REFERENCES

- Gill, A., 1980: Some simple solutions for heat-induced tropical circulation. *Quart. J. Roy. Meteor. Soc.*, **106**, 447–462.
- Hoerling, M., J. Whitaker, A. Kumar, and W. Wang, 2001: The mid-latitude warming during 1998–2000. *Geophys. Res. Lett.*, **28**, 755–758.
- Horel, J., and J. Wallace, 1981: Planetary scale atmospheric phenomena associated with the Southern Oscillation. *Mon. Wea. Rev.*, **109**, 813–829.
- Janowiak, J., and P. Xie, 1999: CAMS–OPI: A global satellite–rain gauge merged product for real-time precipitation monitoring applications. *J. Climate*, **12**, 3335–3342.
- Kalnay, E., and Coauthors, 1996: The NCEP/NCAR 40-Year Reanalysis Project. *Bull. Amer. Meteor. Soc.*, **77**, 437–471.
- Kaplan, A., M. Cane, Y. Kushnir, A. Clement, B. Blumenthal, and B. Rajagopalan, 1998: Analyses of global sea surface temperature 1856–1991. *J. Geophys. Res.*, **103** (C9), 18 567–18 589.
- Martyn, D., 1992: *Climates of the World*. Elsevier, 436 pp.
- Matsuno, T., 1966: Quasi-geostrophic motions in the equatorial area. *J. Meteor. Soc. Japan*, **44**, 24–42.
- Nigam, S., I. Held, and S. Lyons, 1988: Linear simulations of the stationary eddies in a GCM. Part II: The “Mountain” Model. *J. Atmos. Sci.*, **45**, 1433–1452.
- Rasmusson, E. M., and T. H. Carpenter, 1982: Variations in tropical sea surface temperature and surface wind fields associated with the Southern Oscillation/El Niño. *Mon. Wea. Rev.*, **110**, 354–384.
- Ropelewski, C., and M. Halpert, 1987: Global and regional scale precipitation patterns associated with the El Niño/Southern Oscillation. *Mon. Wea. Rev.*, **115**, 1606–1626.
- , and —, 1989: Precipitation patterns associated with the high index phase of the Southern Oscillation. *J. Climate*, **2**, 268–284.
- Trenberth, K., G. Branstator, D. Karoly, A. Kumar, N.-C. Lau, and C. Ropelewski, 1998: Progress during TOGA in understanding and modeling global teleconnections associated with tropical sea surface temperatures. *J. Geophys. Res.*, **103** (C7), 14 291–14 324.